Inorganic Chemistry

ARTICLE

pubs.acs.org/IC

Hydrothermal Synthesis and Crystal Structures of Two Novel Acentric Mixed Alkaline Earth Metal Berylloborates $Sr_3Be_2B_5O_{12}(OH)$ and $Ba_3Be_2B_5O_{12}(OH)$

Colin D. McMillen and Joseph W. Kolis*

Department of Chemistry and Center for Optical Materials Science and Engineering Technologies (COMSET), Clemson University, Clemson, South Carolina 29634-0973, United States

Supporting Information

ABSTRACT: The synthesis and structure of the isostructural acentric compounds $Sr_3Be_2B_5O_{12}(OH)$ (**1**) and $Ba_3Be_2B_5O_{12}(OH)$ (**2**) are reported for the first time. These compounds crystallize in the space group *R*3*m*, and the unit cell parameters are $a = 10.277(15)$ Å and $c = 8.484(17)$ Å for **1** and $a = 10.5615(15)$ Å and $c = 8.8574(18)$ Å for **2**. The structures consist of a network of $[Be_2B_4O_{12}(OH)]$ units interwoven with a network consisting of MO_9 polyhedra (M = Sr, Ba) and BO_3 triangles and exemplify how acentric building blocks such as $[BO_3]^{3-}$, $[BO_4]^{5-}$, and $[BeO_4]^{6-}$ can be especially suitable to build noncentrosymmetric long-range structures. Both networks are centered on the 3-fold rotation axis and present themselves in alternating fashion along [001]. Acentricity is imparted by the alignment of the polarities of BO_3 and BeO_4 environments. Infrared spectroscopy has been used to confirm the local geometries of B and Be, as well as the presence of hydroxide in the crystal structure. Another interesting feature of these compounds is the presence of disorder involving Be and B at the tetrahedral Be site. The degree of the disorder has been confirmed by observing a noticeable shortening of average Be−O bond distances.

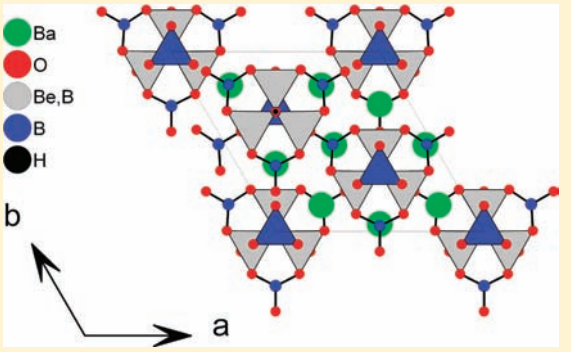

INTRODUCTION

In recent years borates have received attention from researchers studying new and interesting crystal structures as well as those studying materials possessing unique and potentially useful physical and optical properties.[1−8] In terms of their properties, borates tend to possess very wide band gaps (4−9 eV), high optical damage thresholds, and excellent mechanical durability, making them especially suitable for deep-UV optical applications.[5] From a crystallographic standpoint, borates are studied because of the wide variety of structures that can be observed. Boron can adopt either a 3-fold (trigonal planar) or a 4-fold (tetrahedral) coordination with oxygen, leading to a great number of anionic polymeric borate groups including chains, rings, sheets, and framework structures in addition to isolated environments.[2,4]

Borates also have an increased tendency to crystallize in acentric space groups. The percentage of acentric borate structures is over twice that of all reported inorganic structures.[9] A likely reason for this lies in the fact that the most basic structural building blocks of borates, $[BO_3]^{3-}$ and $[BO_4]^{5-}$, lack inversion symmetry themselves. These polar building blocks can act as good starting points for building acentric structures, since they simply need to pack in a fashion where the polarity is aligned to impart noncentrosymmetry. Like boron, beryllium also forms polar coordination environments with oxygen, though trigonal planar environments are far less common for Be.[10]

This tendency to form noncentrosymmetric crystal structures is one of the primary reasons borates and berylloborates are at the center of the search for materials with interesting properties. Nonlinear optical (NLO) susceptibility, piezoelectricity, ferroelectricity, pyroelectricity, and optical activity are all properties that manifest themselves only in materials that lack a center of symmetry.[11] A useful review discussing the space groups of materials that can possess these properties can be found here.[12] Several borates, including β-BaB_2O_4 (BBO),[13] LiB_3O_5 (LBO),[14] $Li_2B_4O_7$,[15] and SrB_4O_7,[16] have received considerable attention by possessing one or more of these unique properties. In the case of NLO susceptibility, additional structure−property relationships have been established for borates on the basis of the anionic groups present in the crystal structure.[17,18] Such work outlining these relationships among the borates helps emphasize the importance of the role of crystallography in materials science.

The introduction of beryllate groups in addition to borates often leads to additional acentric structures such as in $KBe_2BO_3F_2$ (KBBF)[19] and $Sr_2Be_2B_2O_7$ (SBBO).[20] We have previously demonstrated the growth of both KBBF and SBBO crystals hydrothermally.[21,22] In an attempt to optimize the hydrothermal crystal growth of $Sr_2Be_2B_2O_7$ and $Ba_2Be_2B_2O_7$,

Received: April 25, 2011
Published: June 13, 2011

we isolated several new interesting minor products. In this paper, we report the synthesis and crystal structures of two novel hydrated berylloborates that are further examples of the interesting tendency borates have to crystallize without a center of symmetry. The title compounds also exhibit interesting Be/B substitutional disorder that will be discussed in its structural context. Given the unique chemical and physical characteristics of metal borates and beryllates, they seem to be a very promising class of crystals to address the extreme demands of deep-UV optics. Thus, we have developed a detailed explanation of the chemistry of metal berylloborates.

EXPERIMENTAL SECTION

Synthesis. Crystals of the title compounds were obtained using hydrothermal methods from basic aqueous solutions under supercritical conditions. All starting materials were used as-received without further purification. Precious metal reaction ampules were fashioned by crimping and welding the bottom of a 2.5 in. length of 0.25 in. outer diameter silver tubing. The starting materials for each reaction were weighed and placed in the ampule, and 0.4 mL of a 1 M NaOH mineralizer solution was added. The ampule was then welded shut and placed in a Tuttle "cold seal" autoclave having an internal volume of 27 mL. Deionized water was added to fill the remainder of the autoclave's volume, acting as counter-pressure for the reaction vessels. The autoclave was then sealed, placed in a vertical furnace, and heated to 565 °C. The autoclave remained at that temperature for five days, after which it was allowed to cool to room temperature in the furnace over a period of 12 h. The ampules were removed from the autoclave and opened and their contents flushed onto filter paper using deionized water. Clear, colorless, blocklike crystals of the title compounds were obtained as secondary products (approximately 5% yield) and physically separated from the primary products $Sr_2Be_2B_2O_7$ in the case of compound **1** and $BaBe_2B_2O_6$ in the case of compound **2**.

Starting materials for compound **1** were 0.016 g (0.23 mmol) B_2O_3 (Aldrich, 99%), 0.061 g (0.23 mmol) $Sr(OH)_2 \cdot 8H_2O$ (Aldrich, 95%), and 0.006 g (0.24 mmol) BeO (Alfa Aesar, 99%). The starting charge for compound **2** consisted of 0.016 g (0.23 mmol) B_2O_3, 0.082 g (0.48 mmol) $Ba(OH)_2$ (Aldrich, 98%), and 0.006 g (0.24 mmol) BeO. Note that special care should be used to avoid contact with or inhalation of BeO.

Structure Determination. A summary of the structural refinements can be found in Table 1. A single colorless blocklike crystal of compound **1** having dimensions of 0.2 mm × 0.2 mm × 0.2 mm was mounted on a glass fiber using a small amount of epoxy glue. The crystal was centered on a Rigaku AFC8 diffractometer with a Mercury CCD area detector and a graphite monochromated Mo Kα (λ = 0.710 73 Å) radiation source. A total of 2486 reflections were collected at room temperature, 410 of which were unique. Refinement of the crystal structure using a full-matrix least-squares technique was performed using the SHELXTL software package (version 6.1).[23] Initial refinements resulted in R_1 = 0.0312 with a Flack parameter of 0.37(3), suggesting the presence of chiral twinning. As such, this crystal was refined as a chiral twin in the final refinement, and a statistical improvement to R_1 = 0.0249 was noted. The structure of compound **2** was determined in the same manner using a crystal 0.25 mm × 0.25 mm × 0.25 mm in size. For this determination, 2785 total reflections were detected, of which 457 were unique.

In both structures, the location of the hydrogen atom was determined by examining both the local geometries of the oxygen environments and the locations of residual electron density. The position of the hydrogen atom was restrained to an idealized location simply to prevent the O−H bond distance from shortening beyond a reasonable length during subsequent refinements. The partial occupancy of the Be site was determined to be $^2/_3$ Be and $^1/_3$ B in order to achieve charge balance for the compound, and in agreement with bond length observations discussed below.

Table 1. Crystallographic Data for $Sr_3Be_2B_5O_{12}(OH)$ and $Ba_3Be_2B_5O_{12}(OH)$

empirical formula	$Sr_3Be_2B_5O_{12}(OH)$ (**1**)	$Ba_3Be_2B_5O_{12}(OH)$ (**2**)
space group	*R*3*m* (No. 160)	*R*3*m* (No. 160)
a, Å	10.2843(15)	10.5615(15)
c, Å	8.4770(17)	8.8574(18)
V, Å^3	776.5(2)	855.6(2)
Z	3	3
fw	543.94	693.1
density (calcd), Mg/m^3	3.490	4.035
abs coeff, mm^{-1}	15.481	10.313
2θ range, deg	3.32−26.35	3.20−26.30
reflns collected (R_{int})	2486 (0.0465)	2785 (0.0269)
indep reflns	410	457
obsd reflns [$I > 2\sigma(I)$]	408	457
final *R*-indices (obsd data)[a]	R1 = 0.0249, wR2 = 0.0613	R1 = 0.0159, wR2 = 0.0387
R-indices (all data)	R1 = 0.0250, wR2 = 0.0614	R1 = 0.0159, wR2 = 0.0387
GOF on F^2	1.131	1.170
Flack parameter	−10(10)	−0.02(4)
largest difference peak, e/Å^3	0.594	0.369
largest difference hole, e/Å^3	−0.684	−1.000

[a] $R1 = [\Sigma||F_o| - |F_c||]/\Sigma|F^o|$; $wR2 = \{[\Sigma w[(F_o)^2 - (F_c)^2]^2]\}^{1/2}$.

Additional Characterization. Powder X-ray diffraction patterns of well ground crystals of both compounds were measured using a Scintag XDS 2000-2 powder diffractometer with Cu Kα radiation (λ = 1.5418 Å). Patterns were obtained over a 5−65° 2θ range with a step size of 0.03° at 1.0 s/step. These powder patterns were compared to those simulated from the single crystal structure solutions using the Platon for Windows software package.[24]

Infrared spectroscopy was performed using the KBr pellet technique under flowing nitrogen with a Nicolet Magna 550 IR spectrometer. Spectra obtained were the average of 16 scans over a 400−4000 cm^{-1} range with 4 cm^{-1} resolution. The UV band edge of the title compounds (as Supporting Information) was measured from 200 to 1700 nm at a scan rate of 4 nm/s using a Perkin-Elmer Lambda 900 UV−vis−NIR spectrometer. The compounds exhibit the onset of the band edge at about 245 nm, with %*T* dropping to 25% at 220 nm and full absorbance occurring by 201 nm.

RESULTS AND DISCUSSION

Synthesis and Structure Refinement. The title compounds were obtained in fractional yields using the synthetic scheme described above. These crystals were easily distinguishable from the primary products in their respective reactions by their rhombohedral morphology. The largest crystals obtained had edges measuring 0.5 mm in length. Experiments using mineralizers other than 1 M NaOH did not result in any crystals of the title compounds. The starting materials for **1** crystallized as phase pure SBBO from 1 to 4 M NaCl and a mixture of SBBO and $Sr_3B_2O_6$ from 2 to 8 M NaOH. The starting materials for **2** crystallized as $BaBe_2B_2O_6$ and $Ba_2B_5O_9Cl$ from 1 to 4 M NaCl

dx.doi.org/10.1021/ic2008705 |*Inorg. Chem.* 2011, 50, 6809–6813

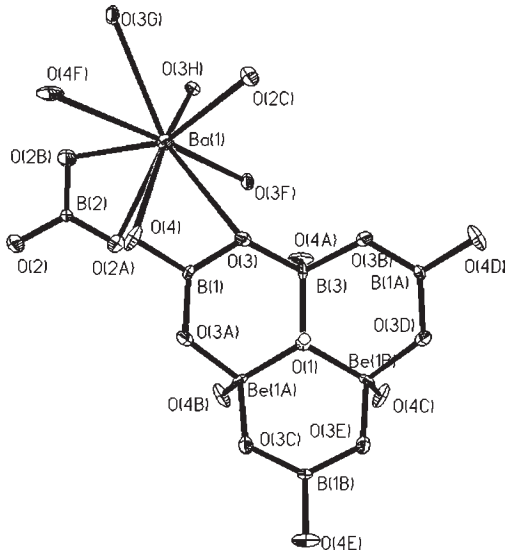

Figure 1. 50% probability thermal ellipsoids plot for $Ba_3Be_2B_5O_{12}(OH)$ viewed just off [001]. The $[Be_2B_4O_{12}(OH)]$ structural building block is found in the lower right portion of the figure.

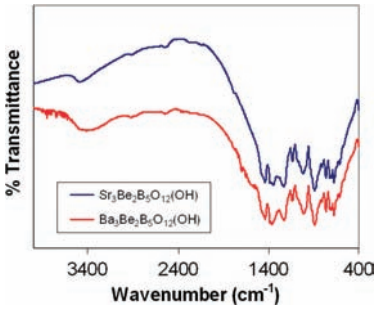

Figure 2. Infrared spectra of the title compounds.

and a mixture of $BaBe_2B_2O_6$ and $BaBO_2(OH)$ from 2 to 8 M NaOH.

The structural details of the title compounds are given in Table 1. Figure 1 is a 50% probability thermal ellipsoids plot for $Ba_3Be_2B_5O_{12}(OH)$, showing an extension of the asymmetric unit to include the local environments for all atoms. The 10% larger volume of the Ba material is directly attributable to the difference between the Shannon radii of Sr and Ba, and, hence, the alkaline earth metal−oxygen bond lengths.[25] Powder XRD patterns simulated from these single crystal structure refinements were identical with experimental patterns obtained from bulk samples of the respective materials.

Infrared Spectroscopy. Infrared spectroscopy can be a useful tool for determining or confirming the geometries of borate groups in solid-state materials. Trigonal planar borates show absorption around 1250−1500 cm^{-1} from asymmetric stretching vibrations, and tetrahedral borates absorb at a frequency of about 850−1100 cm^{-1} for structures that involve both 3- and 4-coordinate boron. Isolated trigonal planar borates tend to have stretching vibrations at slightly lower frequencies (1200−1300 cm^{-1}) than those where both coordination environments are present in combination.[26]

The infrared spectra in Figure 2 are consistent with the borate geometries of the asymmetric unit. The strong band centered at 1345 cm^{-1} corresponds to the trigonal planar B(1)−O stretching vibrations. It is possible that the contribution to this strong absorption at about 1220 cm^{-1} is due to stretching vibrations of the isolated trigonal planar borate environment about B(2) or a B(1)−OH bending mode.[27] The doublet peaks of 886 and 1010 cm^{-1} correspond to tetrahedral B(3)−O stretching vibrations that arise from Be/B disorder at that tetrahedral site. The peaks in the 650−800 cm^{-1} range can likely be attributed to tetrahedral Be(1)−O stretching vibrations from this same site.[27] The IR spectrum also clearly confirms the presence of OH groups in the material by the broad absorption peak centered around 3481 cm^{-1}.

Table 2. Selected Bond Distances (Å), Angles (deg), and Bond Valence (v.u.)[a]

	$Sr_3Be_2B_5O_{12}(OH)$ (1)		$Ba_3Be_2B_5O_{12}(OH)$ (2)	
	dist	BV	dist	BV
M(1)−O(2)^{0}	2.478(5)	0.38	2.571(5)	0.46
M(1)−O(2)^{1,2}	2.646(4) ×2	0.24 ×2	2.758(3) ×2	0.28 ×2
M(1)−O(3)^{3,4}	2.658(4) ×2	0.23 ×2	2.825(3) ×2	0.23 ×2
M(1)−O(3)^{0,5}	2.817(3) ×2	0.15 ×2	2.934(3) ×2	0.17 ×2
M(1)−O(4)^{5,6}	2.713(3) ×2	0.20 ×2	2.851(3) ×2	0.22 ×2
B(1)−O(3)^{0,6}	1.369(5) ×2	1.00 ×2	1.370(4) ×2	1.00 ×2
B(1)−O(4)^{0}	1.388(8)	0.96	1.384(7)	0.96
B(2)−O(2)^{1,2,7}	1.325(5) ×3	1.13 ×3	1.307(4) ×3	1.19 ×3
Be(1)/B(3)−O(1)^{0}	1.512(7)	0.70	1.545(6)	0.64
Be(1)/B(3)−O(3)^{8,9}	1.576(6) ×2	0.59 ×2	1.582(5) ×2	0.58 ×2
Be(1)/B(3)−O(4)^{0}	1.569(10)	0.60	1.567(9)	0.60
O(1)−H(1)	0.940(8)		0.944(6)	
		angle		angle
O(3)−B(1)−O(3)^{6}		125.7(5)		123.0(5)
O(4)−B(1)−O(3)^{0,6}		117.0(3) ×2		118.4(2) ×2
O(2)^{1}−B(2)−O(2)^{2,7}		119.5(2) ×2		119.74(9) ×2
O(2)^{2}−B(2)−O(2)^{7}		119.5(2)		119.74(9)
O(1)−Be(1)/B(3)−O(4)^{0}		110.7(6)		110.1(6)
O(1)−Be(1)/B(3)−O(3)^{8,9}		110.2(4) ×2		110.5(3) ×2
O(3)^{8}−Be(1)/B(3)−O(3)^{9}		107.0(5)		107.1(5)
O(4)−Be(1)/B(3)−O(3)^{8,9}		109.3(3) ×2		109.3(3) ×2
Be(1)/B(3)^{0,5,10}−O(1)−H(1)		97.5(5) ×3		92.0(4) ×3
Be(1)/B(3)−O(1)−Be(1)/B(3)^{5,10}		118.3(2) ×2		119.88(5) ×2
Be(1)/B(3)^{5}−O(1)−Be(1)/B(3)^{10}		118.3(2)		119.88(5)

[a] Symmetry codes: (0) x, y, z; (1) $-x+y+{}^1/_3, -x+{}^5/_3, z-{}^1/_3$; (2) $-y+{}^4/_3, x-y+{}^2/_3, z-{}^1/_3$; (3) $x+{}^1/_3, y+{}^2/_3, z-{}^1/_3$; (4) $x+{}^1/_3, x-y+{}^2/_3, z-{}^1/_3$; (5) $-y+1, x-y+1, z$; (6) $-y+1, -x+1, z$; (7) $x-{}^2/_3, y-{}^1/_3, z-{}^1/_3$; (8) $-x+y+{}^2/_3, y+{}^1/_3, z+{}^1/_3$; (9) $-y+{}^2/_3, x-y+{}^1/_3, z+{}^1/_3$; (10) $-x+y, -x+1, z$.

Crystal Structure. The basic structural building block in the title compounds is a $[Be_2B_4O_{12}(OH)]^{11-}$ polyanion having 3-fold symmetry (lower right portion of Figure 1). Related hexaborate polyanions differing in hydrogen atom location and connectivity have been observed in the structures of a number of naturally occurring hydrated borates described elsewhere.[28−35] The polyanion consists of three rings each composed of two disordered Be/B−O tetrahedra and one triangular planar borate group. The nature of the disorder of the tetrahedral group will be discussed below. Each tetrahedron is shared by two neighboring rings to complete the disordered hexaborate. O(1) is at the center of the building block and shared by each of the tetrahedra. The hydrogen

dx.doi.org/10.1021/ic2008705 |Inorg. Chem. 2011, 50, 6809–6813

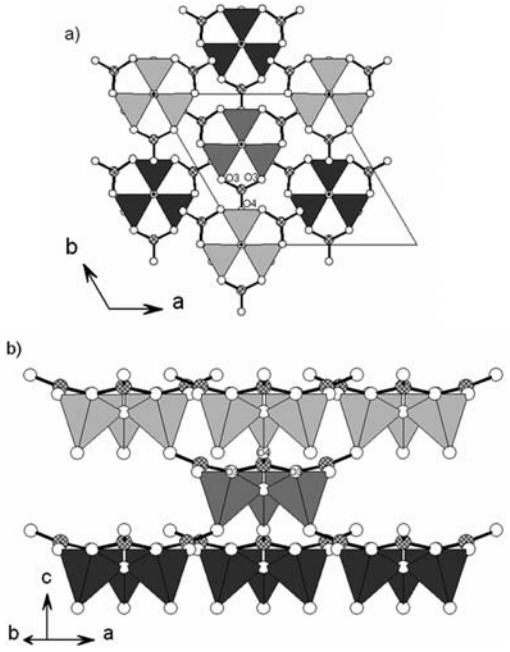

Figure 3. (a) Extended framework of $[Be_2B_4O_{12}(OH)]$ units viewed along [001]. Disordered tetrahedra of the central unit are shaded in medium gray, while those of neighboring units along $+c$ are light gray and $-c$ dark gray in color. Boron atoms are gray with hatching and oxygen atoms are open circles. (b) The same framework viewed slightly off [010]. O(1) bonds to H are white to distinguish them from boron to oxygen bonds (actual H atoms are hidden behind boron atoms).

atom in the structure also connects to O(1) along the 3-fold axis in the [001] direction, forming a triangular pyramid about O(1). This geometry can be inferred from Table 2, which lists selected bond distances and angles for both compounds. The O−H bond distance here is 0.94(1) Å, which is similar to O−H bond distances in structure determinations of other hydrated borates, though there is a large void around this position that could accommodate movement of the H atom farther away from O(1).[35−37]

The $[Be_2B_4O_{12}(OH)]^{11-}$ units exist in layers perpendicular to the *c*-axis in the unit cell. Any given building block is connected to six neighboring building blocks, three each above $(+c)$ and below $(-c)$ it. This connectivity is achieved through B(1) atoms that bridge two O(3) atoms of one $[Be_2B_4O_{12}(OH)]^{11-}$ unit to one O(4) atom on a neighboring polyborate unit in the next higher layer along the *c*-axis. This connection is repeated for all three BO_3 groups that are included in the $[Be_2B_4O_{12}(OH)]^{11-}$ building block. These layers are best seen in Figure 3a, which shows the connectivity from a central building block unit, viewed along [001]. This bridging action among the building blocks gives rise to an extended $[Be_2B_4O_9(OH)]^{3-}$ framework in these materials. The acentric, polar nature of the structure can be seen in the alignment of the Be/B tetrahedra of the building blocks along the *c*-axis in Figure 3b.

There is an additional trigonal orthoborate group that is isolated from these structural building blocks. In this case, the boron atom B(2) is located on a 3*m* symmetry site with three bonds to O(2) atoms, forming a triangular arrangement in the *ab*-plane. Like the tetrahedral site previously mentioned, these BO_3 groups are aligned with respect to each other, causing a net polarity to be imparted in the *ab*-plane as shown in Figure 4. The B(2)−O(2) distances for **1** and **2** are 1.325(5) and 1.307(4) Å, respectively.

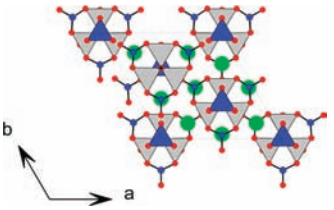

Figure 4. Structure of $Ba_3Be_2B_5O_{12}(OH)$ viewed along [001] including Ba atoms (green). The isolated B2 triangle is shown as a blue polyhedron while the remaining B atoms are blue spheres. Disordered Be tetrahedra are shown as gray polyhedra while oxygen and hydrogen atoms are red and black spheres, respectively.

These bond distances for this borate group are slightly shorter than those about B(1) in this structure, as well as average trigonal planar bond distances in other structures.[4] It is evident that the network of M−O (M = Ba, Sr) bonding holds the B(2) borate group rigidly in place, directing the B−O bonds to be shorter than usual. The alkaline earth metals are 9-coordinate with oxygen and form their own network that is interwoven with that formed by the $[Be_2B_4O_{12}(OH)]^{11-}$ building blocks by sharing O(3) and O(4) atoms. It should be noted that, in both structures, when B(2) is refined as a C atom (that typically form similar planar triangles with short contacts to oxygen, and could have been an impurity ion in the hydroxide precursors), the final *R*-factors became slightly higher (0.0257 for (**1**) and 0.0160 for (**2**)). Thus, charge balance should be achieved only by considering the OH^- group suggested by the infrared analysis and B disorder at the Be site.

Be/B Disorder. One of the interesting features of these crystal structures is a disordered site involving substitution of B atoms for Be. Both Be and B have a strong tendency to form tetrahedral oxyanion fragments. Substitutional disorder involving these elements in oxide systems has been documented in the crystal structures of the naturally occurring minerals rhodizite,[38] gadolinite,[39] calcyberborosilicite,[40] hyalotekite,[41] and hingganite,[42] and the synthetic materials $Y_2Al(BeB)O_7$ ($^1/_2$ occupancy)[43] and $Li_{14}Be_5B(BO_3)_9$ ($^1/_6$ B occupancy).[44] In the title compounds, $^2/_3$ Be and $^1/_3$ B occupancy is observed at the disordered site. The degree of the disorder correlates nicely with the observed bond distances to neighboring oxygen atoms. The site has a tetrahedral coordination to oxygen atoms, with an average bond length of 1.56−1.57 Å. This falls almost exactly $^2/_3$ of the way between accepted distances of 1.48 Å for 4-coordinate B and 1.63 Å for 4-coordinate Be atoms bound to oxygen.[4,10] Similar correlations between interatomic distances and site occupancy have been observed in most of the above cases. Because of the difficulty in detecting light elements by common elemental analysis techniques such as EDX, bond distance arguments are often the only way to determine site occupancy for B/Be disorder. Since crystals of the title compounds were grown in the absence of any other anion, such as fluoride, that could substitute for oxygen and result in shorter bonds to Be, the observed bond distances can be attributed solely to $^1/_3$ B occupancy at the Be site. Most importantly, the disorder implied by these bond distance observations satisfies the overall charge balance of the compounds. The local environments of the oxygen atoms in the structure appear unsuitable to support any additional hydrogen atom assignments beyond that previously discussed for O(1). With this consideration, charge balance can only be achieved through this disordered model.

dx.doi.org/10.1021/ic2008705 |*Inorg. Chem.* 2011, 50, 6809–6813

CONCLUSIONS

Two new acentric beryllborates, $Sr_3Be_2B_5O_{12}(OH)$ and $Ba_3Be_2B_5O_{12}(OH)$, have been synthesized hydrothermally and characterized using X-ray diffraction and infrared spectroscopy. The acentric nature of the structure arises from the aligned polarities of disordered BeO_4 tetrahedra along the *c*-axis and BO_3 triangles in the *ab*-plane. The disorder of B and Be at the tetrahedral site also places these compounds in a unique class with a limited number of oxide-based members. These materials are good examples of how borate and beryllate groups act as suitable building blocks for acentric structures via hydrothermal synthesis.

ASSOCIATED CONTENT

Supporting Information. Additional figure and CIF data. This material is available free of charge via the Internet at http://pubs.acs.org.

AUTHOR INFORMATION

Corresponding Author
*E-mail: kjoseph@clemson.edu.

ACKNOWLEDGMENT

The authors wish to thank the NSF (DMR-0907395) for financial support. We also wish to thank Dr. Bill Pennington and Dr. Don VanDerveer for their structural discussions and insights; and we are grateful for the reviewers' suggestions regarding chiral twinning.

REFERENCES

(1) Christ, C. L.; Clark, J. R. *Phys. Chem. Miner.* **1977**, *2*, 59.
(2) Burns, P. C.; Grice, J. D.; Hawthorne, F. C. *Can. Mineral.* **1995**, *33*, 1131.
(3) Becker, P. *Z. Kristallogr.* **2001**, *216*, 523.
(4) Hawthorne, F. C.; Burns, P. C.; Grice, J. D. *Boron: Mineralogy, Petrology and Geochemistry*; Reviews in Mineralogy; Grew, E. S., Anovitz, L. M., Eds.; Mineralogical Society of America: Washington, DC, 2002; Vol. 33, pp 41−116.
(5) Keszler, D. A. *Curr. Opin. Solid State Mater. Sci.* **1996**, *1*, 204.
(6) Chen, C.; Ning, Y.; Lin, J.; Jiang, J.; Zeng, W.; Wu, B. *Adv. Mater.* **1999**, *11*, 1071.
(7) Sasaki, T.; Mori, Y.; Yoshimura, M.; Yap, Y. K.; Kamimura, T. *Mater. Sci. Eng.* **2000**, *30*, 1.
(8) Chen, C.; Lin, Z.; Wang, Z. *Appl. Phys. B: Lasers Opt.* **2005**, *80*, 1.
(9) Becker, P. *Adv. Mater.* **1998**, *10*, 979.
(10) Hawthorne, F. C.; Huminicki, D. M. C. In *Beryllium: Mineralogy, Petrology and Geochemistry*; Grew, E. S., Ed.; Reviews in Mineralogy and Geochemistry; Mineralogical Society of America: Washington, DC, 2002; Vol. 50, pp 333−403.
(11) Nye, J. F. *Physical Properties of Crystals*, revised ed.; Oxford University Press: New York, 1985.
(12) Halasyamani, P. S.; Poeppelmeier, K. R. *Chem. Mater.* **1998**, *10*, 2753.
(13) Chen, C.; Wu, B.; Jiang, A.; You, G. *Sci. Sinica* **1985**, *B28*, 235.
(14) Chen, C.; Wu, Y.; Jiang, A.; Wu, B.; You, G.; Li, R.; Lin, S. *J. Opt. Soc. Am.* **1989**, *B6*, 616.
(15) Whatmore, R. W.; Shorrocks, N. M.; O'Hara, C.; Ainger, F. W. *Electron. Lett.* **1981**, *17*, 11.
(16) Oseledchik, Y. S.; Prosvirnin, A. L.; Pisarevskiy, A. I.; Starshenko, V. V.; Osadchuk, V. V.; Belokrys, S. P.; Svitanko, N. V.; Korol, A. S.; Krikunov, S. A.; Selevich, A. F. *Opt. Mater.* **1995**, *4*, 669.
(17) Xue, D.; Betzler, K.; Hesse, H. *Solid State Commun.* **2000**, *114*, 21.
(18) Xue, D.; Betzler, K.; Hesse, H. *OSA Trends Opt. Photonics Ser.* **2000**, *34*, 542.
(19) Chen, C.; Lu, J.; Togashi, T.; Suganuma, T.; Sekikawa, T.; Watanabe, S.; Xu, Z.; Wang, J. *Opt. Lett.* **2002**, *27*, 637.
(20) Chen, C.; Wang, Y.; Wu, B.; Wu, K.; Zeng, W.; Yu, L. *Nature* **1995**, *373*, 322.
(21) McMillen, C. D.; Kolis, J. W. *J. Cryst. Growth* **2008**, *310*, 2033.
(22) Kolis, J. W.; McMillen, C. D.; Franco, T. *Mater. Res. Soc. Symp. Proc.* **2005**, *848*, 3.
(23) Sheldrick, G. M. *SHELXTL Version 6.1, Program for Crystal Structure Refinement*; University of Gottingen: Gottingen, Germany, 2000.
(24) Spek, A. L. *PLATON—A Multipurpose Crystallographic Tool*; Utrecht University: Utrecht, The Netherlands, 2003.
(25) Shannon, R. D.; Prewitt, C. T. *Acta Crystallogr., Sect. B.* **1970**, *26*, 1046.
(26) Ross, S. D. In *The Infrared Spectra of Minerals*; Farmer, V. C., Ed.; Mineralogical Society Monograph 4;Mineralogical Society: London, 1974; pp 205−226.
(27) Weir, C. E. *J. Res. Natl. Bur. Stand. (U.S.)* **1966**, *70A*, 153.
(28) Grice, J. D. *Can. Mineral.* **2005**, *43*, 1019.
(29) Dal Negro, A.; Ungaretti, L.; Sabelli, C. *Am. Mineral.* **1971**, *56*, 1553.
(30) Dal Negro, A.; Ungaretti, L. *Naturwissenschaften* **1973**, *60*, 350.
(31) Dal Negro, A.; Sabelli, C.; Ungaretti, L. *Atti. Accad. Naz. Lincei, Cl. Sci. Fis., Mat. Nat., Rend.* **1969**, *47*, 353.
(32) Ghose, S.; Wan, C. *Am. Mineral.* **1977**, *62*, 979.
(33) Clark, J. R.; Applemen, D. E.; Christ, C. L. *J. Inorg. Nucl. Chem.* **1964**, *26*, 73.
(34) Brovkin, A. A.; Zayakina, N.; Brovkina, V. S. *Kristallografiya* **1975**, *20*, 911.
(35) Burns, P. C.; Hawthorne, F. C. *Can. Mineral.* **1994**, *32*, 895.
(36) Burns, P. C.; Hawthorne, F. C. *Can. Mineral.* **1994**, *32*, 533.
(37) Barbier, J.; Park, H. *Can. Mineral.* **2001**, *39*, 129.
(38) Pring, A.; Din, V. K.; Jefferson, D. A.; Thomas, J. M. *Mineral. Mag.* **1986**, *50*, 163.
(39) Demartin, F.; Pilati, T.; Diella, V.; Gentile, P.; Gramaccioli, C. M. *Can. Mineral.* **1993**, *30*, 127.
(40) Rastsvetaeva, R. K.; Pushcharovskii, D. Y.; Pekov, I. V.; Voloshin, A. V. *Kristallografiya* **1996**, *41*, 235.
(41) Christy, A. G.; Grew, E. S.; Mayo, S. C.; Yates, M. G.; Belakovskiy, D. I. *Mineral. Mag.* **1998**, *62*, 77.
(42) Demartin, F.; Minaglia, A.; Gramaccioli, C. M. *Can. Mineral.* **2001**, *39*, 1105.
(43) Kuz'micheva, G. M.; Rybakov, V. B.; Kutovoi, S. A.; Panyutin, V. L.; Oleinik, A. Y.; Plashkarev, O. G. *Neorg. Mater.* **2002**, *38*, 72.
(44) Luce, J. L.; Shaffers, K. I.; Keszler, D. A. *Inorg. Chem.* **1994**, *33*, 2453.